Calibration of 2D and 3D Track Models for Simulation of Vehicle–track Interaction and Differential Settlement in Transition Zones Using Field

Calibration of 2D and 3D Track Models for Simulation of Vehicle–track Interaction and Differential Settlement in Transition Zones Using Field Measurement Data

Kourosh Nasrollahi[1](✉), Ana Ramos[2], Jens C. O. Nielsen[1], Jelke Dijkstra[3], and Magnus Ekh[4]

[1] Department of Mechanics and Maritime Sciences/CHARMEC, Chalmers University of Technology, SE-412 96, Gothenburg, Sweden
kourosh.nasrollahi@chalmers.se
[2] CONSTRUCT – LESE, Faculty of Engineering, University of Porto, Porto, Portugal
[3] Department of Architecture and Civil Engineering, Chalmers University of Technology, Gothenburg, Sweden
[4] Department of Industrial and Materials Science, Chalmers University of Technology, Gothenburg, Sweden

Abstract. A comparison of two models of vertical dynamic vehicle–track interaction in a transition zone between a ballasted track and a 3MB slab track is presented. The dynamic analysis is performed using 2D and 3D models in MATLAB and ANSYS, respectively. The Kelvin-Voigt model representing the foundation for the sleeper in the 2D model is calibrated based on the calculated track receptance from the more extensive 3D model, which includes the track superstructure on a layered soil foundation. Both models are used to simulate the passage of an iron ore freight vehicle through the transition zone at 60 km/h. Sleeper vertical displacements, sleeper–ballast contact forces and wheel–rail contact forces are compared. Both models show results for similar orders of magnitude. The simulation time is about 25 times shorter for the 2D model.

Keywords: Transition zone · differential settlement model · dynamic vehicle–track interaction · 2D and 3D models · calibration

1 Introduction

In transition zones between two different track forms, there is a discontinuity in track structure leading to a gradient in track stiffness [1–5]. Examples include transitions between different superstructures, e.g., slab track to ballasted track, and/or between different substructures, e.g., embankment to a bridge or tunnel structure. Further, differences in loading and support conditions at the interfaces between track superstructure and substructure on either side of the transition may lead to differential track settlement and an irregularity in longitudinal rail level soon after construction. This results in

W. Huang and M. Ahmadian (Eds.): IAVSD 2023, LNME, pp. 711–720, 2025.
https://doi.org/10.1007/978-3-031-66971-2_74

an amplification of the dynamic traffic loading along the transition, contributing to the degradation process of ballast and subgrade and resulting in a further deterioration of vertical track geometry. Hence, the track adjacent to a transition is prone to deteriorate at an accelerating rate, and frequent maintenance work may be required. In recent years, infrastructure managers and researchers have dedicated great attention to the understanding and optimisation of the long-term performance of transition zones using both simulation models and field measurements, see e.g. [6].

Various models for the simulation of dynamic vehicle–track interaction and differential settlement have been applied for analyses of transition zone performance. The type and complexity of the model influence how reliable and accurate the analysis of the vehicle–track interaction is. Various assumptions and requirements need to be considered: the type of the required analysis (static or dynamic), linear or non-linear analysis (for example including material plasticity and voided sleepers), computational cost, and the requested outputs. An extensive review on models of dynamic vehicle–track interaction in transition zones and their applications can be found in [7, 8]. However, few numerical models have been calibrated and validated versus field measurements.

In 2022–2023, an extensive field measurement campaign was carried out in a transition zone on the Swedish heavy-haul line Malmbanan [9–11]. The transition zone is between a conventional ballasted track and a 3MB "Moulded Modular Multi-Blocks" slab track. The applied fibre Bragg grating-based (FBG) long-term monitoring arrangement, with a high temporal resolution, was prepared for both short-term and long-term condition monitoring of an operational railway track in harsh conditions in the north of Sweden. With reference to the measured results, this paper compares two models for time-domain simulation of vertical dynamic vehicle–track interaction in a transition zone. For a single loaded iron ore vehicle passage at 60 km/h, simulated time histories of wheel–rail contact forces and sleeper vertical displacements are compared with the corresponding responses measured in the transition.

Ramos et al. [12] studied the short- and long-term behaviour of ballasted and slab tracks subjected to cyclic loading. Settlements of both track forms were compared using laboratory experiments and calibrated numerical models. The two track forms were subjected to three million cycles of loading using an iterative approach. The calculated settlements were used to develop and calibrate the short-term response of three-dimensional (3D) finite element (FE) models of both track structures. In [2], the same 3D FE model integrated with an empirical settlement model was used to analyse a transition zone between slab track on an embankment and slab track in a tunnel. Contact elements were used to simulate voids between the slab's hydraulically bound layer and the frost protection layer. In each iteration, the calculated 3D stress field in the substructure was used as input in the settlement model to compute settlement along the transition. These settlements were used to modify the 3D model geometry in the subsequent iteration.

In Nasrollahi et al. [5], a methodology for the simulation of long-term differential track settlement, the development of voided sleepers leading to a redistribution of rail seat loads, and the evolving irregularity in vertical track geometry at a transition between two track forms, is presented. For a prescribed traffic load, the accumulated settlement is predicted using an iterative approach. A time-domain model of vertical dynamic vehicle–track interaction using a two-dimensional (2D) FE model is applied to calculate the contact forces between sleepers and ballast in the short term. These are used in an empirical model to determine the long-term settlement of the ballast/subgrade below each sleeper. Gravity loads and state-dependent track conditions are accounted for, including a prescribed variation of non-linear stiffness of the supporting foundation along the track model.

2 Track and Vehicle Models

The measured dynamic responses are compared to results from simulations with two alternative FE models in 2D and 3D, respectively. These models are used for time-domain simulation of vertical dynamic vehicle–track interaction in a transition zone between two different track forms see Fig. 1. In the following, the models are briefly described and compared to the measurements.

The first model is a reduced-order representation of the transition zone [2], see Fig. 1(a). Symmetric loading with respect to a vertical plane along the track centre is assumed leading to that only half of the track (and vehicle) is considered. The track model is a non-linear 2D FE model using beam elements for the rail and for the top blocks and base in the slab track. Each rigid sleeper is supported by a state-dependent discrete spring and viscous damper model of the foundation. The model accounts for the variation and redistribution of supporting loads between adjacent sleepers that occur over time due to accumulated settlement and the potential development of voided sleepers. However, the interaction between sleepers via the ground is neglected. Input to the foundation model is provided from the 3D FE model, see below. The dynamic vehicle–track interaction is simulated using the in-house software DIFF, while the empirical settlement model is based on a visco-plastic material formulation implemented in MATLAB.

The second model uses solid finite elements in an extensive 3D representation of superstructure, ballast and soil in the transition [3], see Fig. 1(b). The parameter values for the 3D track model are presented in Table 1. Symmetry conditions as in the 2D model are adopted and the simulation of dynamic vehicle–track interaction is carried out using the software ANSYS. Hanging sleepers or voids between slab and foundation are considered using contact elements [3]. From each simulation, the stresses in all finite elements of the geomaterials are obtained. These are used as input to an empirical permanent deformation model to simulate the differential settlement of the soil. The influence of the number of load cycles, initial stress state, stresses induced by the passage of the train and strength properties of the materials are accounted for.

In Fig. 1, the total length of each track model is 40 m (corresponding to 25 m of ballasted track and 15 m of slab track). In the 2D model, each sleeper in the ballasted track section is modelled by one discrete (rigid) element with one vertical degree of freedom (DOF) and mass $m_s = 150$ kg. Uniform sleeper distance $L = 0.6$ m is assumed.

The two-layer slab track is modelled by one continuous beam representing the base slab below a layer of discrete blocks. Rail properties are labelled with index'r'. The two layers of the 3MB slab track are labelled 't.b' and 'b.b', respectively. Each layer of Euler-Bernoulli beam elements has bending stiffness *EI* and mass *m* per unit beam length, width *b* and height *h*. The connection between each pair of adjacent nodes in the different layers is modelled as a spring and viscous damper in parallel. Input data for the track model can be found in [5].

In the 3D model, similar/equivalent properties are adopted to make the two models as consistent as possible. As in the 2D model, the rail is modelled with Euler-Bernoulli beam elements and each rail pad with a spring-damper element. Regarding the remaining materials, all of them are modelled as linear elastic using solid (brick) elements with eight nodes, which is a good compromise in terms of simulation time and expected accuracy. Moreover, the adopted mesh was defined to optimize the computational cost and accuracy. Thus, based on a convergence study, the results in terms of displacements and stresses from the different mesh resolutions were successfully compared. The distance between the symmetry plane at the centre of the track model and the opposite boundary (plane *yx*) on the field side is close to 6 m.

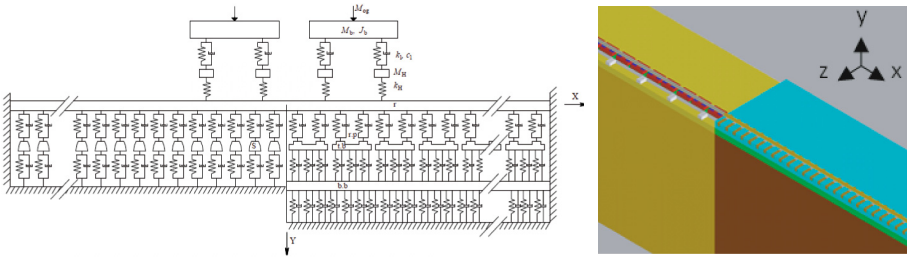

Fig. 1. Sketches of transition zone models: (a) 2D model, (b) 3D model

Rayleigh damping was applied for the 3D model. For the concrete materials and the geomaterials, relative dampings $\xi = 0.01$ and $\xi = 0.03$ were assumed, respectively. The corresponding α and β coefficients were determined based on a specified range of frequencies (5–200 Hz). To avoid spurious wave reflections from the vertical boundaries of the geomaterials (*xy* plane), viscous dampers were adopted using the Lysmer formulation. Indeed, this approach has been used in the scope of 3D modelling with good results, see [10]. On the horizontal boundary at the bottom of the model (*xz* plane), fixed supports were adopted for both track forms. On the remaining boundaries, viscous dampers (in all directions) were applied for the geomaterials. The dynamic analysis was performed in the software ANSYS using the Newmark-Raphson method with a fixed time step of 0.005s (sampling frequency 200 Hz).

Table 1. Parameters of the 3D model

Substructure	Superstructure		
Ballast	$E = 67.5$ MPa	Concrete Slab	$E = 30$ GPa
	$\nu = 0.20$		$\nu = 0.20$
	$\rho = 1800$ kg/m^3		$\rho = 2500$ kg/m^3
	$\alpha = 1.84$		$\alpha = 0.61$
	$\beta = 4.66 \times 10^{-5}$		$\beta = 1.55 \times 10^{-5}$
Sub-ballast	$E = 161.7$ MPa	Block	$E = 30$ GPa
	$\nu = 0.30$		$\nu = 0.20$
	$\rho = 2100$ kg/m^3		$\rho = 2500$ kg/m^3
	$\alpha = 1.84$		$\alpha = 0.61$
	$\beta = 4.66 \times 10^{-5}$		$\beta = 1.55 \times 10^{-5}$
Soil layer 1	$E = 472.5$ MPa	Resilient Mat	$E = 2.5 \times 10^5$ Pa
	$\nu = 0.25$		$\nu = 0.40$
	$\rho = 2100$ kg/m^3		$\rho = 2000$ kg/m^3
	$\alpha = 1.84$		$\alpha = 3.06$
	$\beta = 4.66 \times 10^{-5}$		$\beta = 7.76 \times 10–5$
Soil layer 2	$E = 800$ MPa	Sleepers	$E = 38$ GPa
	$\nu = 0.25$		$\nu = 0.15$
	$\rho = 2100$ kg/m^3		$\rho = 2500$ kg/m^3
	$\alpha = 1.84$		
	$\beta = 4.66 \times 10^{-5}$		

Table 2. Parameter values for vehicle model with axle load 31.5 tonnes

$M_\mathrm{b} = 800$ kg	$J_\mathrm{b} = 730$ kg m^2	$M_\mathrm{w} = 1341$ kg	$J_\mathrm{w} = 100$ kg m^2
$\Delta_w = 1.78$ m	$\Delta_b = 1.74$ m	$k_1 = 30$ MN/m	$c_1 = 70$ kNs/m
$k_2 = 3.75$ MN/m	$c_2 = 10$ kNs/m	$M_{og} = 29.8$ tonnes	

In this study, the vehicle model contains two bogies from two adjacent iron ore wagons, see Fig. 1(a). An alternative vehicle model, see [5], including two bogies and a carbody is also considered. Each bogie is modelled by six DOFs with primary suspension stiffness k_1 and damping c_1, and secondary suspension stiffness k_2 and damping c_2. In both models, linearised Hertzian wheel–rail contact stiffness $K_{\mathrm{H}i} = 1.07$ kN/mm, $i = 1, 2, 3,$ and 4) is assumed. The weight of half of the car body is accounted for by a static point-load acting at the centroid of the bogie. The nominal axle load of the iron ore wagons is 30 tonnes, but according to wheel impact load detector data there are

significant variations in axle load [10]. The speed of loaded trains is 60 km/h. The parameter values for the vehicle model presented in Table 2 were collected from [5].

3 Field Measurements

A setup for real-time condition monitoring was developed and implemented to assess the influence of traffic load on accumulated differential settlement in a transition zone, see [9, 10]. Based on FBG technology, the instrumentation for in-situ long-term condition monitoring of track bed degradation was developed and implemented to provide data for verification and calibration of the simulation model. The system was designed for measurements in an operational railway track in harsh conditions in the north of Sweden. The instrumentation along the transition comprises four clusters, each with an optical strain gauge array on the rail web in one sleeper bay, and an accelerometer and a displacement transducer on the sleeper. Two additional accelerometers were installed far from the transition zone to measure a reference state. Combined, the data should not only provide details on long-term differential settlement, but also the change in dynamic response it underpins. Condition monitoring of the transition zone commenced on 15th of September 2022 and continued until 15th of June 2023. The early measurements focused on calibrating and evaluating the monitoring setup for measuring the dynamic response and permanent deformations of the track during the passage of individual loaded iron ore trains. In this paper, only the short-term measurements are considered for the calibration of the models.

4 Comparison of 2D and 3D Models

4.1 Track Receptance

The 2D and 3D model representations of the ballasted track (excluding the slab track in the model) are first assessed by comparing their rail receptances. Both the excitation and the response are evaluated on the rail above a railseat. Frequencies from 0 Hz up to 500 Hz are studied. Magnitudes of receptances from the different models are presented in Fig. 2. The 3D model with the more detailed representation of the layered foundation displays (at least) two resonances up to 150 Hz. This cannot be captured with the simplified description of the foundation in the 2D model. Thus, the stiffness and damping of the sleeper support in the 2D model were tuned so that the static receptance and its fundamental resonance occur in a similar frequency range and with a similar magnitude. A reasonable match between the 2D and 3D models is achieved if the sleeper foundation stiffness and damping in the 2D model are 60 kN/mm and 80 Ns/mm, respectively.

The 2D track model has two resonances and one antiresonance in the studied frequency range. At the first resonance frequency 70 Hz, the sleeper and rail move in phase, while they move out of phase at the second resonance frequency 320 Hz. The second resonance is in good agreement with the 3D model.

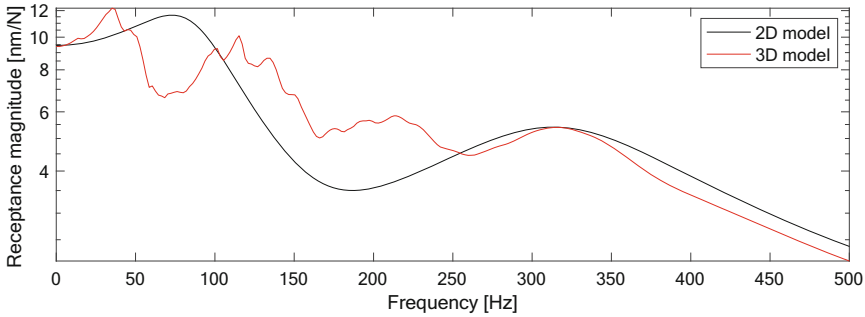

Fig. 2. Comparison of direct rail receptance above a sleeper between the 2D and 3D models.

4.2 Short-Term Dynamic Response

The influence of the stiffness gradient between the two different track forms, and accounting for a non-uniform initial misalignment (dip) in rail level on the ballasted side in the 2D model (initial misalignment will be considered in the 3D model in future work) on various short-term dynamic responses on the ballasted side is evaluated.

Figure 3 shows the time history of the calculated wheel–rail contact force for the leading wheel of the leading bogie. The results from the 2D and 3D track models are compared with wheel–rail contact force data measured in four sleeper bays (sleeper bays 3, 5, 8, and 11 numbered from the slab track). To analyse the influence of the low-frequency pitching motion of the car body induced by the stiffness gradient and rail misalignment, the full vehicle model is compared with the simplified vehicle model consisting of two bogies from two adjacent vehicles. Based on the simulation, it is confirmed that the stiffness gradient at the transition leads to a minor contribution to the dynamic load, while the influence of the track irregularity is more significant, cf. [5]. Further, it is possible to observe that the 3D model can capture the magnitude of the measured train-track interaction force at some instances. The measured wheel–rail contact forces present a more significant variation in magnitude from one span to another. This can be because of an in-situ variation in support conditions from one sleeper to the next, whereas in the simulation a uniform foundation has been assumed [9]. In the 2D model, different voids (dip) for sleepers 1 to 11 have been assumed based on measured settlements of corresponding sleepers [9]. For example, sleeper number 1 is assumed to have a void of 3 mm, while sleeper 11 has a void of 0.1 mm. The sleepers between these two have voids ranging from 0.1 to 3 mm.

In Fig. 4, measured and simulated sleeper displacements are compared. Further, simulated sleeper–ballast contact forces are compared in Fig. 5. Train speed 60 km/h and axle load 31.5 tonnes have been assumed. As discussed in [5, 9], wheel–rail contact forces are higher at the transition. This leads to higher sleeper–ballast contact forces and sleeper displacements as shown in Fig. 4. The calculated sleeper displacements obtained from the 2D model are found to be essentially consistent with the measured data. As can be observed from Fig. 5(a), the sleeper–ballast contact force generated due to passage of four wheels from two bogies in two adjacent iron ore wagons form a sequence of four equidistant wheel loads.

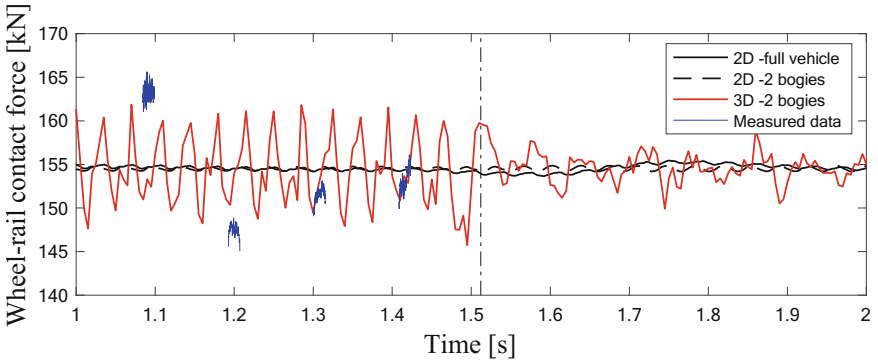

Fig. 3. Time history of vertical wheel–rail contact force for the leading wheelset for the 2D and 3D models. Comparison with measured wheel–rail contact forces in sleeper bays 3, 5, 8, and 11. Transition between two track forms is indicated by the vertical black dash-dotted line.

In general, both the 3D and 2D models are capable of successfully representing the dynamic response of the transition zone. The 3D model is more comprehensive and advanced as it incorporates the modelling of the layered subgrade and accounts for any other movements occurring in the transition zone in the superstructure (ballast and above elements). On the other hand, the 2D model is considered sufficient for calculating dynamic responses and long-term simulation in shorter time. It's worth mentioning that while the 3D model provides a more detailed representation of the system, it may also require more computational resources and time compared to the 2D model. Therefore, the choice between these models depends on the specific requirements of the analysis, including the desired level of accuracy and available computational capabilities.

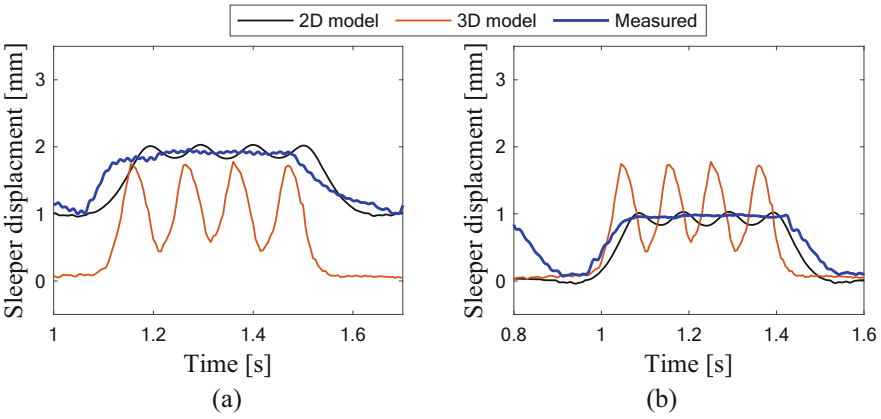

Fig. 4. Measured and calculated sleeper displacements using the 2D and 3D models: (a) sleeper 3 and (b) sleeper 11. For the 3D model, the displacement was calculated at railseat. In the 2D model, different voids for sleepers 3 and 11 have been prescribed based on measured settlements [9].

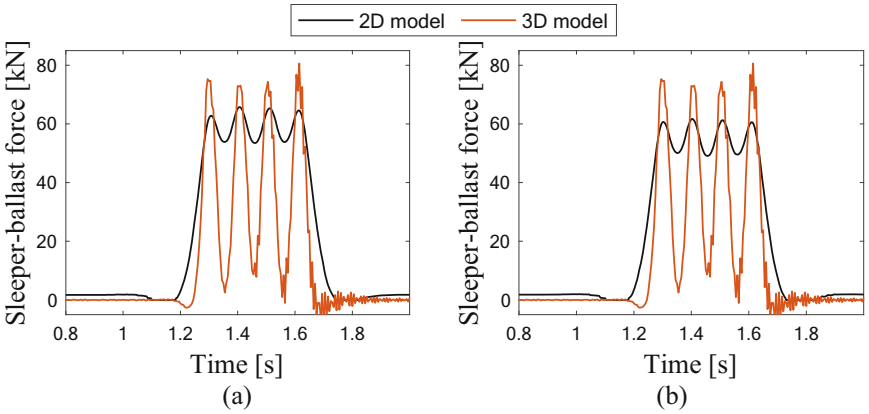

Fig. 5. Calculated sleeper–ballast contact forces using the 2D and 3D models: (a) sleeper 3 and (b) sleeper 11. In the 2D model, different voids for sleepers 3 and 11 have been prescribed based on measured settlements [9].

5 Conclusions

This paper presents two approaches for the modelling of the dynamic response of a transition zone between two railway track forms. As both track models are based on the finite element method, numerical efficiency is an important factor leading to the need for different simplifications in the models. In the 2D FE model, the computational demand is significantly lower than for the 3D model at the expense of a very much more simplified representation of the foundation.

The stiffness and damping of the foundation in the 2D model were tuned by comparing the rail receptances of the 2D and 3D models. Both models capture the same orders of magnitude as the measured wheel–rail contact forces and sleeper displacements (and sleeper–ballast contact forces). This implies that both models can successfully represent the dynamic response of the transition zone, but a further assessment of the observed differences in results between the two models is necessary for improved understanding before guidelines on transition zone modelling can be presented. Concerning the measurements, these include the in-situ variation in support conditions for adjacent sleepers and any other irregularities in the track. A substantial simplification in the 2D model is the assumption of non-interacting springs and viscous dampers for several layers of the track.

Acknowledgement. The current study is part of the ongoing activities in CHARMEC – Chalmers Railway Mechanics (www.chalmers.se/charmec). Parts of the study have been funded from the European Union's Horizon 2020 research and innovation programme in the projects In2Track2 and In2Track3 under grant agreements Nos 826255 and 101012456. This work was also partly financed by FCT/MCTES through national funds (PIDDAC) under the R&D Unit CONSTRUCT – Institute of R&D in Structures and Construction, under reference UIDB/04708/2020. Parts of the simulations were performed using resources at Chalmers Centre for Componential Science and Engineering (C3SE) provided by the Swedish National Infrastructures for Computing (SNIC).

References

1. Aggestam, E., Nielsen, J.C.O.: Multi-objective optimisation of transition zones between slab track and ballasted track using a genetic algorithm. J. Sound Vib. **446**, 91–112 (2019)
2. Ramos, A., Gomes Correia, A., Calçada, R., Connolly, D.P.: Ballastless railway track transition zones: an embankment to tunnel analysis. Transp. Geotech. **33**, 100728 (2022)
3. Wang, H., Markine, V.: Modelling of the long-term behaviour of transition zones: prediction of track settlement. Eng. Struct. **156**, 294–304 (2018)
4. Shan, Y., et al.: Iterative method for predicting uneven settlement caused by high-speed train loads in transition-zone subgrade. Transp. Res. Rec. **2607**, 7–14 (2017)
5. Nasrollahi, K., Nielsen, J.C.O., Aggestam, E., Dijkstra, J., Ekh, M.: Prediction of long-term differential track settlement in a transition zone using an iterative approach. Eng. Struct. **283**, 115830 (2023)
6. Dahlberg, T.: Railway track stiffness variations - consequences and countermeasures. Int. J. Civil Eng. **8**, 1–12 (2010)
7. Indraratna, B., Babar Sajjad, M., Ngo, T., Gomes Correia, A., Kelly, R.: Improved performance of ballasted tracks at transition zones: a review of experimental and modelling approaches. Transp. Geotech. **21**, 100260 (2019)
8. Sañudo, R., Dell'Olio, L., Casado, J.A., Carrascal, I.A., Diego, S.: Track transitions in railways: a review. Constr. Build. Mater. **112**, 140–157 (2016)
9. Nasrollahi, K., Dijkstra, J., Nielsen, J.C.O.: Towards real-time condition monitoring of a transition zone in a railway structure using fibre Bragg grating sensors. Transp. Geotech. **44**, 101166 (2024)
10. Nasrollahi, K., Dijkstra, J., Nielsen, J.C.O., Ekh, M.: Long-term monitoring of settlements below a transition zone in a railway structure. In: Proceedings of the 11th International Symposium on Field Monitoring in Geomechanics, ISFMG 2022, 4–7 September 2022, London, United Kingdom (2022)
11. Nasrollahi, K.: Differential railway track settlement in a transition zone – field measurements and numerical simulations (Licentiate thesis). Chalmers University of Technology, Department of Mechanics and Maritime Sciences, Division of Dynamics, Gothenburg, Sweden (2023)
12. Ramos, A., et al.: Influence of track foundation on the performance of ballast and concrete slab tracks under cyclic loading: physical modelling and numerical model calibration. Constr. Build. Mater. **277**, 122245 (2021)